Sensors and Materials, Vol. 34, No. 6 (2022) 2253–2262
MYU Tokyo

S & M 2970

Using Software to Simulate Effect of Stacking Order of High- and Low-refractive-index Materials on Properties of Distributed Bragg Reflector

Ke-Hua Chen,[1] Wei Chien,[2*] Cheng-Fu Yang,[3,4**] and Ning Wu[5]

[1]College of Information and Mechanical & Electrical Engineering, Ningde Normal University, Ningde, Fujian 352100, China
[2]Department of School of Electric and Information Engineering, Beibu Gulf University, Qinzhou 535000, China
[3]Department of Chemical and Materials Engineering, National University of Kaohsiung, Kaohsiung 811, Taiwan
[4]Department of Aeronautical Engineering, Chaoyang University of Technology, Taichung 413, Taiwan
[5]Advanced Science and Technology Research Institute, Beibu Gulf University, Qinzhou 535000, China

(Received December 30, 2021; accepted April 5, 2022)

Keywords: stacking effect, overall transfer matrix, COMSOL, simulation, SiO_2–Ta_2O_5 reflector, different periods

In this study, we used an e-beam evaporation method to deposit SiO_2 and Ta_2O_5 single-layer films on glass substrates, then the extinction coefficients (k values) and refractive indices (n values) of the deposited films were measured using a thin-film analyzer in the range of 300–1000 nm. The k values of the SiO_2 and Ta_2O_5 single-layer films were almost zero in the measured range and the n values decreased slightly with increasing light wavelength. The measured n values of the SiO_2 and Ta_2O_5 single-layer films were used to design a green-wavelength distributed Bragg reflector (DBR) with a central wavelength of 550 nm. The thicknesses (d) of the SiO_2 and Ta_2O_5 single-layer films for the quarter wavelength ($\lambda/4$) for green light (550 nm) were calculated using $d = \lambda/(4n)$ to be 94.17 and 64.55 nm, respectively. Next, the measured n values and the calculated thicknesses of the SiO_2 and Ta_2O_5 single-layer films were incorporated into the overall transfer matrix (OTM) investigated by ourselves, and COMSOL Multiphysics® software was used to calculate and simulate the reflectance spectra of the designed green-light DBR with two, four, and six periods. Sheppard's approximate equation was also used to calculate the maximum reflectance ratios of the designed green-light DBR, and the calculated values were compared with those obtained by OTM and COMSOL simulations. We discuss the reasons for the differences between these calculated results.

1. Introduction

A distributed Bragg reflector (DBR) can be designed and fabricated using periodic structures of alternating oxide or semiconductive films, and can achieve a high ratio of reflection (over 95%) within a designed range of light wavelengths. DBRs can be designed to reflect arbitrary

*Corresponding author: e-mail: air180@seed.net.tw
**Corresponding author: e-mail: cfyang@nuk.edu.tw
https://doi.org/10.18494/SAM3831

ISSN 0914-4935
https://myukk.org/

light wavelengths by changing the used film materials or the thicknesses of the films. DBRs can be designed and investigated for different applications, such as photonic passive and active devices. Shanmugan *et al.* designed a high-reflectivity DBR mirror and used a plasma-enhanced chemical vapor deposition system to deposit Si_3N_4–SiO_2 bilayer films (with thicknesses of 170 nm and 255 ± 20 nm) in the fabrication of a DBR. The stacked Si_3N_4–SiO_2 bilayer films had high reflectivity and were incorporated in a novel structure entirely comprising dielectric-based mirrors that could be used to tune resonant cavity devices in a MEMS configuration.[1]

A DBR can also be used to improve the efficiency of light collection in full angle Lambertian emission because it can focus the wavelength-converter-based light source to a smaller angle.[2] Zhou *et al.* designed an organic cavity to form standing waves between grating pixels for laser emission, in which the gratings behaved similarly to an in-plane selective mirror. Then, they used this structure to fabricate an active cavity sensor based on an organic DBR laser.[3] Veldhuis *et al.* deposited Si_3N_4–SiO_2 bilayer films as an optical channel waveguide, and they investigated and integrated the optical DBR device as a chemo-optical sensor to sense water–ethanol mixtures.[4] Lee *et al.* investigated a DBR with multilayer structures to measure the 2D surface pressure profile across the device for dynamic load sensing.[5] These studies demonstrate that DBRs can be applied as sensors of different materials or physical properties. Bilayer-film structures are used in many commercial DBRs, for example, single-period structures of L(Al_2O_3)/H(TiO_2), L(MgF_2)/H(Nb_2O_5), and L(SiO_2)/H(TiO_2), and different numbers of periods can be used.[6–8] Sheppard investigated the following approximate equation to calculate the maximum reflectance ratios of DBRs with different materials (i.e., different refractive indices or n values) and different periods:[9]

$$R = \left[\frac{(n_H)^{2p} - (n_0 / n_S)(n_L)^{2p}}{(n_H)^{2p} + (n_0 / n_S)(n_L)^{2p}} \right]^2. \tag{1}$$

In this study, SiO_2 and Ta_2O_5 single-layer films were used as low- (n_L) and high-refractive-index (n_H) materials, respectively, and Corning Gorilla glass was used as the substrates (n_S). Therefore, n_L, n_H, and n_S at 550 nm were 2.158, 1.460, and 1.518, respectively, and n_0 was 1, i.e., that for air. R and P are the maximum reflectance ratio at the wavelength of the reflectance light and the stacking period of the designed SiO_2–Ta_2O_5 bilayer DBR, respectively. However, the equation investigated by Sheppard can only be used to simulate and find the maximum reflectance ratio of the designed DBR at a certain wavelength, and it cannot simulate the reflectance spectra of the designed DBR in a specified range of light wavelengths. Sheppard's approximate equation has been used in many studies to calculate the reflectance ratios of designed DBRs, and the obtained results were recognized as the maximum values for the designed multilayer films at a specific wavelength. However, to our knowledge, simulation results have not been compared with results calculated using Sheppard's approximate equation. Also, the following equation has been investigated to calculate the reflectance bandwidth at a specified central wavelength of a designed DBR:[10]

$$\frac{\Delta\lambda}{\lambda}=\left(4/\pi\right)\arcsin\left[\frac{n_H-n_L}{n_H+n_L}\right], \tag{2}$$

where $\Delta\lambda$ and λ are the reflectance bandwidth at the designed reflectance wavelength and the central reflectance wavelength of the designed DBR, respectively. Also, we can find no reports of comparisons of simulation results with the reflectance bandwidth calculated using Eq. (2).

Many simulation methods for designing a multilayer DBR with optimized properties have been investigated. COMSOL Multiphysics® (COMSOL) is a very useful simulation software package for simulating and analyzing the electromagnetic and optical properties of a single-layer film or multilayer films with different stacking orders. COMSOL can also be used to find the optimum thicknesses of multilayer stacked films giving the best characteristics. For example, Xu *et al.* used COMSOL to simulate a designed red-light DRB with a central wavelength of 700 nm.[11] They found the optimum thicknesses of all the stacked films, which they used to design a DBR with a small full width at half maximum (FWHM). Also, the passband of the designed DBR had high reflectance and low ripple intensities, and the ripple intensities outside the reflectance band were small. We previously incorporated the calculated thicknesses of SiO_2 and Nb_2O_5 films and the measured *n* values of each layer into an overall transfer matrix (OTM), which we used to simulate and calculate the reflectance spectra of newly designed SiO_2-Nb_2O_5 bilayer DBRs.[12]

In this study, we used two different simulation methods to simulate the reflectance spectra of designed SiO_2–Ta_2O_5 bilayer DBRs. The *n* values of SiO_2 and Nb_2O_5 films were incorporated into the investigated OTM and COMSOL to simulate the reflectance spectra. We then compared the simulation results of the designed SiO_2–Ta_2O_5 bilayer DBRs with the maximum reflectance ratios calculated using Sheppard's approximate equation, which can calculate the maximum reflectance ratio of a specific wavelength. Then, the possible bandwidth was calculated using Eq. (2). Finally, we discuss the reason for the differences between the simulation and calculation results.

2. Simulation Process and Parameters

To incorporate the *n* values of SiO_2 and Ta_2O_5 films into the investigated OTM and COMSOL as low- and high-refractive-index films, respectively, to design a multilayer green-light DBR on Corning 1737 glass substrates, it was first necessary to deposit the films and measure their properties. Therefore, after cleaning 2 × 2 cm^2 Corning 1737 glass substrates, an e-beam was used to deposit single-layer SiO_2 and Ta_2O_5 films on the substrates. A chamber base pressure of 6×10^{-6} Torr was used to start the deposition of the SiO_2 and Ta_2O_5 films. The deposition parameters were a voltage of 4 kV and a current of 20 mA, and the deposition was performed at room temperature (25 °C). We used a film gauge to control the thicknesses of the deposited SiO_2 and Ta_2O_5 films to about 80 nm. A thin-film analyzer was used to measure the extinction coefficients (*k* values) and *n* values of SiO_2 and Ta_2O_5 single-layer films.

Two, four, and six stacking periods were used for the designed SiO_2–Ta_2O_5 DBR as shown in Fig. 1. Two different structures of the SiO_2–Ta_2O_5 multilayer films were used to design the DBR for the simulation. The first was a high-low (HL) stacking structure, in which a Ta_2O_5 film was first deposited on the glass substrate, and then a SiO_2 film was deposited on the Ta_2O_5 film (Fig. 1(a)). The second was a low-high (LH) stacking structure, in which a SiO_2 film was first deposited on the glass substrate, and then a Ta_2O_5 film was deposited on the SiO_2 film [Fig. 1(b)].

The relationship between the electrical field (E_a) and magnetic field (H_a) is written as the following matrix equation:[13,14]

$$\begin{bmatrix} E_a \\ H_a \end{bmatrix} = \begin{bmatrix} \cos\delta & \frac{i}{N}\sin\delta \\ iN\sin\delta & \cos\delta \end{bmatrix} \begin{bmatrix} E_b \\ H_b \end{bmatrix}, \tag{3}$$

where δ represents the phase factor and is expressed as

$$\delta = 2\pi\, Nd\cos(\theta)/\lambda. \tag{4}$$

Here, d and N are the thickness and the complex index (which is equal to $nr - ikr$) of the used film, λ is the central wavelength of the designed DBR, and n and k are the n and k values of the used film, respectively. N is a modified optical admittance of the deposited film given by

$$N = \vec{E}/\vec{H}. \tag{5}$$

For the multilayer films, when an electromagnetic wave (including light) penetrates from the front air layer or a reference plane to each layer of the multilayer films and then to the substrate, the input optical admittance for the single layer and for two ($P = 2$, four layers), four ($P = 4$, eight layers), and six periods ($P = 6$, twelve layers) are respectively expressed as

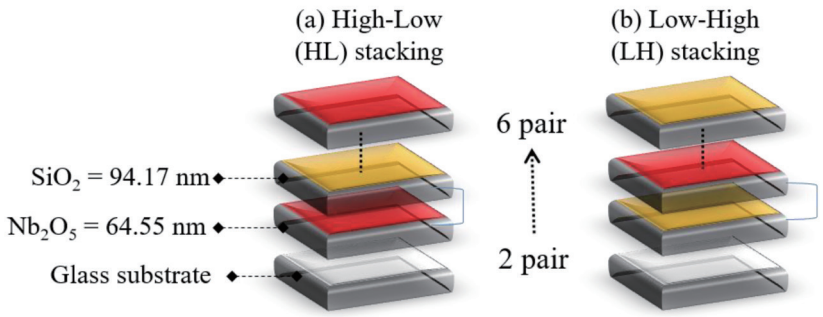

Fig. 1. (Color online) Structures of two differently designed SiO_2–Ta_2O_5 bilayer films with different periods: (a) HL stacking structure and (b) LH stacking structure.

$$\begin{bmatrix} B_1 \\ C_1 \end{bmatrix} = \begin{bmatrix} \cos\delta_1 & \frac{i}{N}\sin\delta_1 \\ iN\sin\delta_1 & \cos\delta_1 \end{bmatrix} \begin{bmatrix} 1 \\ y_s \end{bmatrix}, \; Y_1 = \frac{B_1}{C_1} \text{ for } P = 1, \tag{6}$$

$$\begin{bmatrix} B_4 \\ C_4 \end{bmatrix} = \begin{bmatrix} \cos\delta_4 & \frac{i}{N}\sin\delta_4 \\ iN\sin\delta_4 & \cos\delta_4 \end{bmatrix} \begin{bmatrix} 1 \\ Y_3 \end{bmatrix}, \; Y_4 = \frac{B_4}{C_4}, \text{ and } R = |\rho|^2 = \frac{|Y_0 - Y_4|^2}{|Y_0 + Y_4|^2} \text{ for } P = 2, \tag{7}$$

$$\begin{bmatrix} B_8 \\ C_8 \end{bmatrix} = \begin{bmatrix} \cos\delta_8 & \frac{i}{N}\sin\delta_8 \\ iN\sin\delta_8 & \cos\delta_8 \end{bmatrix} \begin{bmatrix} 1 \\ Y_9 \end{bmatrix}, \; Y_8 = \frac{B_8}{C_8}, \text{ and } R = |\rho|^2 = \frac{|Y_0 - Y_8|^2}{|Y_0 + Y_8|^2} \text{ for } P = 4, \tag{8}$$

$$\begin{bmatrix} B_{12} \\ C_{12} \end{bmatrix} = \begin{bmatrix} \cos\delta_{12} & \frac{i}{N}\sin\delta_{12} \\ iN\sin\delta_{12} & \cos\delta_{12} \end{bmatrix} \begin{bmatrix} 1 \\ Y_{11} \end{bmatrix}, Y_{12} = \frac{B_{12}}{C_{12}}, \text{ and } R = |\rho|^2 = \frac{|Y_0 - Y_{12}|^2}{|Y_0 + Y_{12}|^2} \text{ for } P = 6, \tag{9}$$

where y_s is the admittance of the substrate. The variations in the reflectance properties of the bilayer SiO_2–Ta_2O_5 Bragg reflectors were simulated using the investigated OTM and COMSOL. The simulated results were compared with the maximum reflectance ratio calculated using Sheppard's approximate equation and the reflectance bandwidth calculated from Eq. (2).

3. Simulation Results and Discussion

To investigate the performances of the two different simulation tools used to calculate the reflectance spectra of the designed SiO_2–Ta_2O_5 bilayer DBRs, the following steps were carried out. First, the single-layer SiO_2 and Ta_2O_5 films were deposited on glass substrates using the e-beam evaporation system. Next, a thin-film analyzer was used to measure the *k* and *n* values of SiO_2 and Ta_2O_5 single-layer films, their *n* values measured at 550 nm were incorporated into the equation $d = \lambda/(4n)$, and the thicknesses required to match the $\lambda/4$ SiO_2 and Ta_2O_5 films were obtained. Third, the OTM was used to simulate the multilayer films and calculate the reflective spectra of bilayer SiO_2–Ta_2O_5 DBRs with different periods by incorporating the measured *n* values of SiO_2 and Ta_2O_5 single-layer films. Fourth, models with different periods of bilayer SiO_2–Ta_2O_5 Bragg reflectors were constructed in COMSOL, then the measured *n* values of the SiO_2 and Ta_2O_5 single-layer films were incorporated into COMSOL to calculate the reflective spectra of the designed DBRs. Finally, the simulation properties of the bilayer SiO_2–Ta_2O_5 DBRs obtained from the OTM simulation and COMSOL were compared with the maximum reflectance ratios obtained from Sheppard's approximate equation and the reflectance bandwidth obtained from Eq. (2).

The *k* and *n* values of the single-layer SiO_2 and Ta_2O_5 films were measured as a function of the light wavelength as shown in Fig. 2. The *k* values of the single-layer SiO_2 and Ta_2O_5 films were almost zero in the light wavelength range of 300–1000 nm. Therefore, they were recognized

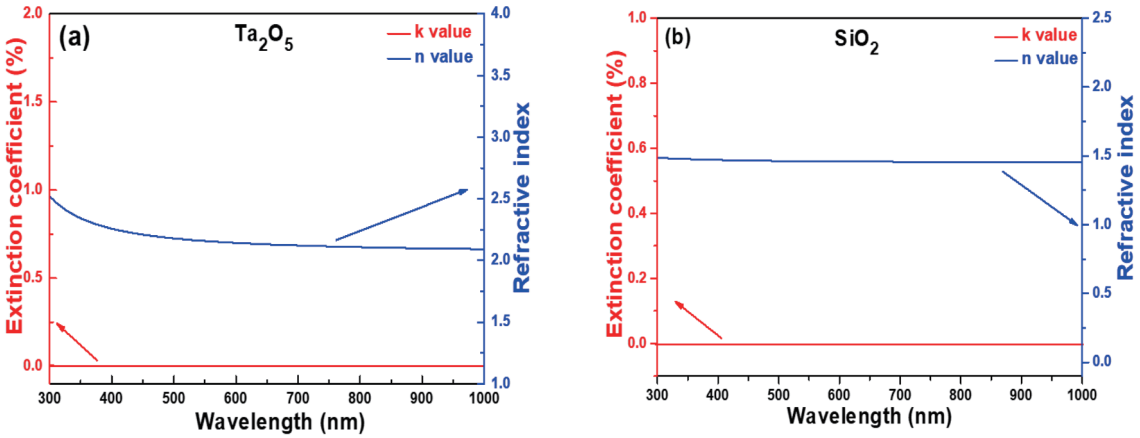

Fig. 2. (Color online) Measured k and n values of (a) single-layer SiO_2 and (b) single-layer Ta_2O_5 films.

as lossless dielectric films, and the k values of the single-layer SiO_2 and Ta_2O_5 films were recognized as having no effect on the reflectance properties of the designed DBRs. The n values of the single-layer SiO_2 and Ta_2O_5 films were not fixed and decreased slightly with increasing light wavelength. As shown in Fig. 2(a), the n value of the Ta_2O_5 film was 2.522 at 300 nm and decreased slightly with increasing light wavelength. The n values of the Ta_2O_5 film were 2.258, 2.158, and 2.121 at light wavelengths of 400, 550, and 700 nm, respectively, but the n value did not significantly change above a light wavelength of 700 nm. As shown in Fig. 2(b), the n values of the SiO_2 film were 1.486, 1.470, 1460, and 1.456 at light wavelengths of 300, 400, 550, and 700 nm, respectively, and the n value showed little change with increasing light wavelength.

The n values of the SiO_2 film and glass substrate were lower than that of the Ta_2O_5 film at all measured wavelengths. Therefore, the SiO_2 film was used as a low-refractive-index film and the Ta_2O_5 film was used as a high-refractive-index film to design a multilayer green-light DBR. The n values of the SiO_2 and Ta_2O_5 single-layer films at the light wavelength of 550 nm were 1.460 and 2.158, respectively. We used the equation $d = \lambda/(4n)$ to calculate the thicknesses of the SiO_2 and Ta_2O_5 films that matched the designed quarter wavelength, where the n values were 1.460 and 2.158 for the SiO_2 and Ta_2O_5 films, respectively, and λ was the central wavelength of 550 nm. The calculated thicknesses of the SiO_2 and Ta_2O_5 films were 94.17 and 64.55 nm, respectively.

Because the designed green-light DBRs had a central wavelength of 550 nm, the n values of the SiO_2 and Ta_2O_5 films at 550 nm were 1.460 and 2.158, respectively, which were incorporated into Sheppard's approximate equation [Eq. (1)] to find the optimum reflectance ratios for the DBRs with two, four, and six periods. The measured results gave maximum reflectance ratios of the SiO_2–Ta_2O_5 bilayer DBRs with two, four, and six periods of 55.26, 87.81, and 97.17%, respectively. Next, the n values of 1.460 and 2.158 were incorporated into the approximate equation [Eq. (2)] to obtain a reflectance bandwidth of 136 nm at the central wavelength for the designed SiO_2–Ta_2O_5 bilayer DBRs. Because both the SiO_2 and Ta_2O_5 films were lossless dielectric films, the variation of the n values shown in Fig. 2 could be used to simulate the reflectance spectra of the designed DBRs shown in Fig. 1. Here, SiO_2–Ta_2O_5 bilayer films with

SiO_2 and Ta_2O_5 single-layer films of 94.17 and 64.55 nm thicknesses, respectively, were used to simulate the designed DBRs with two, four, and six periods.

The reflectance spectra of the designed SiO_2–Ta_2O_5 bilayer DBR calculated using the investigated OTM in the light wavelength range of 350–800 nm are compared in Fig. 3 as a function of stacking order and period number. To find the effects of both the stacking order and the period number of the SiO_2 and Ta_2O_5 films on the reflectance spectra, the theoretical results were calculated by incorporating the variation of the n values shown in Fig. 2 and the same thicknesses of the SiO_2 and Ta_2O_5 films (94.17 and 64.55 nm) into the calculations for the OTM given by Eqs. (7)–(9). As shown in Fig. 3, both the stacking order and the period number had a large effect on the reflectance spectra of the designed SiO_2–Ta_2O_5 bilayer DBRs. The simulation results of the designed DBRs with a central wavelength of 550 nm and different stacking orders and period numbers are compared in Table 1 in terms of the maximum reflectance ratio (MaxR, %), the wavelength giving the maximum reflectance ratio (Wave, nm), the central wavelength of the reflectance bandwidth (CWave, nm), the reflectance bandwidth (BD, defined as the range accounting for 90% of the maximum reflectance ratio, nm), and the FWHM.

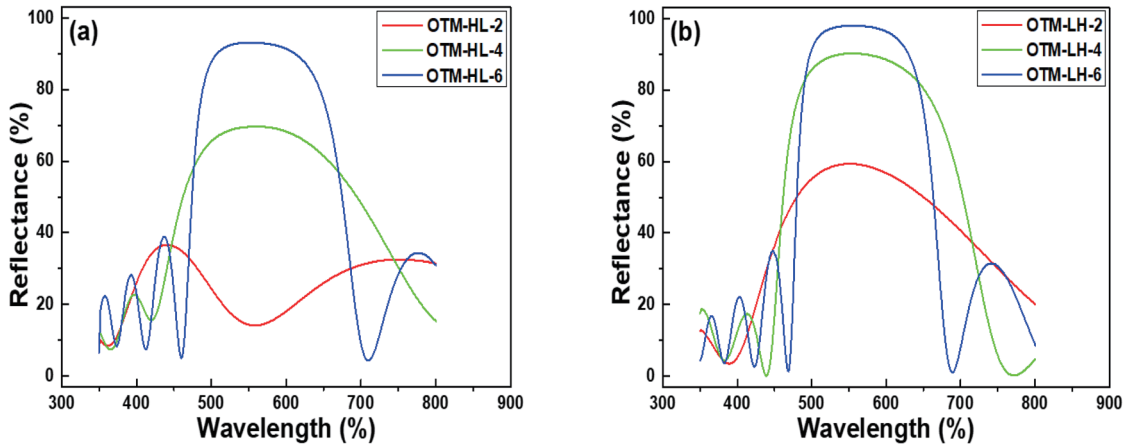

Fig. 3. (Color online) Results of the designed green-light DBR simulated with the investigated OTM as a function of period number (a) using the HL stacking structure and (b) using the LH stacking structure shown Figs. 1(a) and 1(b), respectively.

Table 1
Results of the designed green-light DBR simulated with the investigated OTM for different numbers of periods. The designed central wavelength was 550 nm. MaxR: maximum reflectance ratio (%), Wave: wavelength of maximum reflectance ratio (nm), BD: bandwidth (nm), CWave: central wavelength (nm), FWHM: full width at half maximum (nm).

	HL stacking structure (periods)			LH stacking structure (periods)		
Periods	2	4	6	2	4	6
MaxR	—	69.6	93.1	59.3	90.2	98.0
Wave	—	560	551	552	553	553
BD	—	154	144	137	159	139
CWave	—	566	565	563	568	564
FWHM	—	294	204	314	248	183

As shown in Fig. 3 and Table 1, except for the OTM-HL-2 spectrum, all the simulation reflectance spectra had a similar trend in the light wavelength range of 350–800 nm. For the DBR with the OTM-HL-2 structure, two reflectance peaks centered at 416 and 750 nm were observed, and no reflectance peak centered at 550 nm was observed. When the number of stacking periods of the OTM-HL structure was increased from two to four and six, a reflectance peak centered at about 550 nm was observed. As the period number of the OTM-HL structure increased from four to six, MaxR increased from 69.6 to 93.1%, Wave shifted from 560 to 551 nm, BD decreased from 154 to 144 nm, CWave shifted from 566 to 565 nm, and the FWHM decreased from 294 to 204 nm. However, for the DBR with the OTM-LH-2 structure, one reflectance peak centered at about 550 nm was observed. As the period number of the OTM-LH structure increased from two to six, Wave of MaxR shifted from 552 to 553 nm, MaxR increased from 59.3 to 98.0%, BD changed in the range of 137–159 nm, CWave changed in the range of 563–568 nm, and the FWHM markedly decreased from 314 to 183 nm.

As shown in Fig. 4 and Table 2, the COMSOL-simulated results of the designed SiO_2–Ta_2O_5 bilayer DBRs were similar to those obtained by OTM simulation. Except for the COMSOL-

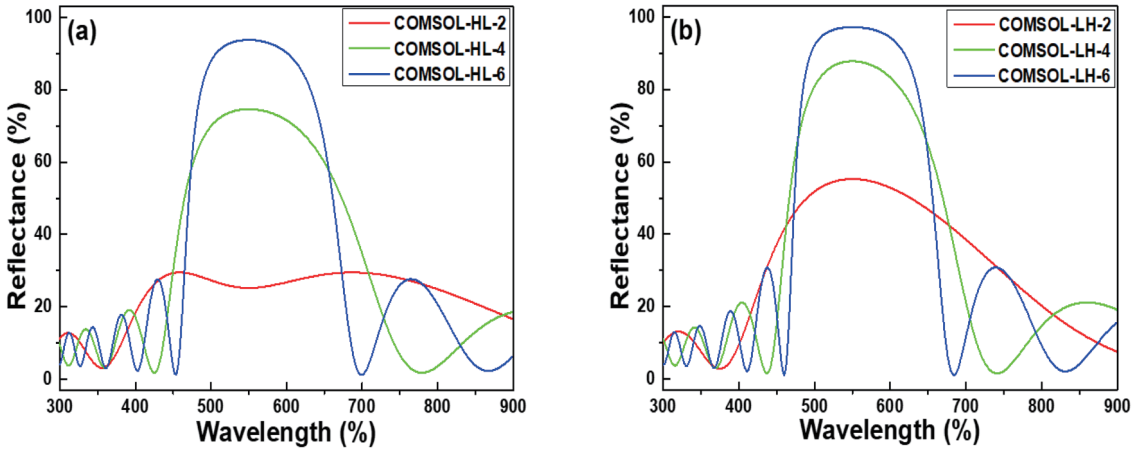

Fig. 4. (Color online) Results of the designed green-light DBR simulated with COMSOL as a function of period number (a) using the HL stacking structure and (b) using the LH stacking structure shown in Figs. 1(a) and 1(b), respectively.

Table 2
Results of the designed green-light DBR simulated with COMSOL for different numbers of periods. The designed central wavelength was 550 nm. MaxR: maximum reflectance ratio (%), Wave: wavelength of maximum reflectance ratio (nm), BD: bandwidth (nm), CWave: central wavelength (nm), FWHM: full width at half maximum (nm).

	HL stacking structure (periods)			LH stacking structure (periods)		
Periods	2	4	6	2	4	6
MaxR	—	74.6	93.7	55.3	87.8	97.2
Wave	—	550	549	550	550	550
BD	—	134	129	140	121	132
CWave	—	557	557	559	556	558
FWHM	—	241	193	325	213	184

HL-2 structure, all the simulation reflectance spectra had a similar trend in the light wavelength range of 300–900 nm. Also, the DBR with the COMSOL-HL-2 structure had two reflectance peaks centered at 498 and 702 nm, and no reflectance peak centered at 550 nm was observed. Also, as the number of stacking periods of the COMSOL-HL structure increased from two to four and six, the reflectance peak centered at about 550 nm was observed. As the period number of the OTM-HL structure increased from four to six, MaxR increased from 74.6 to 93.7%, Wave shifted from 550 to 549 nm, BD decreased from 134 to 129 nm, CWave remained at 557 nm, and the FWHM decreased from 241 to 193 nm. For the DBR with the COMSOL-LH-2 structure, one reflectance peak centered at about 550 nm was observed. As the period number of the COMSOL-LH structure increased from two to six, MaxR increased from 55.3 to 97.2%, Wave remained at 550 nm, BD changed in the range of 121–140 nm, CWave changed in the range of 556–559 nm, and the FWHM markedly decreased from 325 to 184 nm.

The results in Figs. 3 and 4 show that the stacking order and period number strongly affect the properties of the designed SiO_2–Ta_2O_5 bilayer DBRs. As the investigated OTM and COMSOL are used to simulate the designed SiO_2–Ta_2O_5 bilayer DBR with the HL-2 structure, it cannot have the properties of a DBR. This is because the Ta_2O_5 film is stacked on the glass substrate first and because the glass substrate has a lower n value than the Ta_2O_5 film and a value close to that of the SiO_2 film. The function of the first stacked Ta_2O_5 film will be eliminated, the first stacked SiO_2–Ta_2O_5 bilayer films cannot work as the reflective films, and the first SiO_2 film will interfere with the reflection of light because of the reflection of light by the second stacking SiO_2–Ta_2O_5 bilayer films. Therefore, the ideal stacking period for the HL-2 structure for ensuring reflectance of the bilayer films is only one, and this structure cannot form a DBR. However, if the LH-2 structure is used to design the DBR, the low-refractive-index SiO_2 film will shield the interference effect of the glass substrate and form a period with the first Ta_2O_5 film to ensure the reflection of light. Therefore, the LH-2 structure can act as a DBR.

Using Eq. (1), we found that the stacked SiO_2–Ta_2O_5 bilayer films with three and five periods had maximum reflectance ratios of 77.6 and 94.8%, respectively. These two values are close to the two simulation values for the HL-4 and HL-6 structures in Tables 1 and 2, respectively. These results validate our hypothesis that the number of periods in the SiO_2–Ta_2O_5-glass stacking structure should be decreased by one to ensure the reflection of light. These results also reveal the important finding that Sheppard's approximate equation only applies to the LH stacking structure and not to the HL stacking structure. When glass is used as the substrate, to apply Sheppard's approximate equation to the HL stacking structure, the period number P must be adjusted. As we have shown, P for the HL-4 and HL-6 structures should be changed from 4 and 6 to 3 and 5, respectively. Comparison of Tables 1 and 2 shows that when the different simulation methods are used to simulate the HL stacking structure, the trends of the simulation results are close to those calculated by Sheppard's approximate equation and Eq. (2). These results suggest that the two simulation tools can help determine the reflectance properties of bilayer DBRs.

4. Conclusions

In this study, we successfully used the investigated OTM and COMSOL numerical analysis software to simulate designed DBRs with different periods and stacking orders of SiO_2–Ta_2O_5 bilayer films. Despite some differences between the simulation and calculated results, the trends of the simulation results were close to the results calculated by Sheppard's approximate equation and Eq. (2). We also showed that the stacking order of the high- and low-dielectric-index films had a strong effect on the reflectance properties of the designed bilayer DBRs. When glass was used as the substrate and the high-refractive-index film was stacked first, the period number P needed to be adjusted. For example, P for the HL-4 and HL-6 structures should be changed from 4 and 6 to 3 and 5, respectively.

Acknowledgments

This work was supported by projects under Nos. MOST 110-2622-E-390-002 and MOST 110-2221-E-390-020.

References

1 V. Shanmugan, M. A. Shah, S. L. Teo, and A. Ramam: Proc. MEMS/MOEMS Technologies and Applications II; Photonics Asia 5641 (Beijing, China, 2004).
2 B. Gao, J. P. George, J. Beeckman, and K. Neyts: Opt. Express **28** (2020) 12837.
3 Z. Zhou, W. Qiao, Q. Wang, L. Chen, and W. Huang: J. Mater. Chem. C **6** (2018) 2565.
4 G. J. Veldhuis, J. H. Berends, R. G. Heideman, and P. V. Lambeck: Pure Appl. Opt. **7** (1998) L23.
5 G. Lee, David A. Scripka, B. Wagner, N. N. Thadhani, Z. Kang, and C. J. Summers: Opt. Express **25** (2017) 27067.
6 J. Liu, C. Y. Lin, W. C. Tzou, N. K. Hsueh, C. F. Yang, and Y. Chen: Cryst. Growth Design **18** (2018) 5426.
7 Y. Du, B. S. Chen, J. J. Lin, H. W. Tseng, Y. L. Wu, and C. F. Yang: Modern Phys. Lett. B **35** (2021) 2140001.
8 V. Pervak, S. Naumov, G. Tempea, V. Yakovlev, F. Krausz, and A. Apolonski: Proc. SPIE **5963** (2005) 59631P.
9 C. J. R. Sheppard: Pure Appl. Opt. J. Eur. Opt. Soc. A**4** (1995) 665.
10 T. H. Chang, T. E. Lee, N. K. Hsueh, C. H. Lin, and C. F. Yang: Microsyst. Technol. **24** (2018) 3941.
11 J. Xu, C. H. Lin, Y. T. Chen, H. W. Tseng, P. Wang, C. F. Yang, and C. L. Lin: Sens. Mater. **33** (2021) 2619.
12 Z. S. Yuan, J. M. Jhang, P. H. Yu, C. M. Jiang, Y. C. Huang, Y. L. Wu, J. J. Lin, and C. F. Yang: Vacuum **13** (2020) 109782.
13 H. A. Macleod: Thin-Film Optical Filters (McGraw-Hill, New York, 1985) 2nd ed.
14 Y. C. Chen, C. F. Yang, and E. Y. Hsueh: J. Electrochem. Soc. **157** (2010) H987.